Polyhedron 52 (2013) 810–819

Contents lists available at SciVerse ScienceDirect

Polyhedron

journal homepage: www.elsevier.com/locate/poly

Convenient in situ generation of a chiral bis-*N*-heterocyclic carbene palladium catalyst and its application in enantioselective synthesis

Amrita B. Mullick, Matthew S. Jeletic, Andrew R. Powers, Ion Ghiviriga, Khalil A. Abboud, Adam S. Veige *

University of Florida, Center for Catalysis, P.O. Box 117200, Gainesville, FL 32611, USA

ARTICLE INFO

Article history:
Available online 9 August 2012

Dedicated to Alfred Werner on the 100th Anniversary of his Nobel Prize in Chemistry in 1913.

Keywords:
Carbene
Catalyst
In situ
Chiral
Enantioselective
Asymmetric

ABSTRACT

To simplify catalytic reactions employing chelating bisNHC–metal complexes, studies were conducted to elucidate conditions for the in situ generation of a chiral chelating bisNHC–palladium catalyst from the corresponding diimidazolium salt. The method provides a convenient entry to catalytic reactions and eliminates catalyst preparation steps. In addition to the in situ prepared catalyst, for comparative purposes, isolable species were synthesized and characterized by NMR spectroscopy, combustion analysis, and single-crystal X-ray diffraction. Employing C_2-symmetric ligands derived from *trans*-9,10-Dihydro-9,10-EthanoAnthracene-11,12-diyl (DEA) and *trans*-9,10-Dihydro-9,10-EthanoAnthracene-11,12-diyl-Methanediyl (DEAM), diNHC–Pd complexes were synthesized and tested for activity in enantioselective arylboronic acid addition to cyclic enones.

Published by Elsevier Ltd.

1. Introduction

One of the most exciting advances in homogeneous metal-mediated catalysis over the past decade is the emergence of *N*-heterocyclic carbene (NHC) ligands [1–11]. The rapid rise in application of NHC ligands is due in part to numerous fundamental studies that probe important NHC–metal properties including: size/volume [12–16], π-acidity [17–27], σ-donating strength [14–16,21,22,28–43], and flexibility [44–47]. Exploiting this wealth of data permits the design of highly refined ligands and, in the area of metal-catalyzed asymmetric catalysis [48], ligands capable of producing products in high enantiomeric excess (% e.e.) [44,49–70]. Creating a useful chiral catalyst involves more than simply achieving high enantioselectivity; a catalyst must be easy to use and inexpensive to prepare. One disadvantage to employing a NHC ligand is that catalysts are typically preformed and stored prior to use. Many ligands, including the class of C_2-symmetric "privileged ligands" [71], can simply be added to a metal catalyst precursor to generate the active species in situ. This method offers several distinct advantages over the use of preformed catalysts; for example it: (1) facilitates benchtop chemistry, (2) boasts the ability to rapidly screen a wide scope of metal ion precursors, (3) avoids additional catalyst synthetic steps, (4) prevents potential loss of catalyst integrity from long-term storage, and (5) solves the potential problem that active catalysts can be difficult to isolate.

A few examples of in situ generated mono-NHC metal catalysts have been reported. Nolan and co-workers demonstrate the utility of in situ generated NHC–metal catalysts in Suzuki, Kumada, and Sonogashira couplings [72–75]. Employing a chelating diphosphorous ligand, Minnaard and co-workers demonstrate the competence of in situ generated catalysts in the asymmetric conjugate addition of arylboronic acids to enones [76], a reaction important for creating chiral centers [77–80], which is primarily catalyzed by copper- and rhodium-based catalysts [81–87]. The catalyst can be generated in one pot containing the ligand, a base, and a metal precursor. Upon addition of reagents, catalysis proceeds yielding enantio-enriched product.

Mono- and diNHC supported palladium complexes catalyze Michael addition reactions [57]. Our group [44,57,65,88–91] and several others have developed diNHC ligands and employed them in metal-mediated asymmetric catalysis [49–70,92–103]. Specifically, our focus centers on exploiting chiral C_2-symmetric ligands derived from *trans*-9,10-**D**ihydro-9,10-EthanoAnthracene-11,12-diyl (DEA) and *trans*-9,10-Dihydro-9,10-EthanoAnthracene-11,12-diylMethanediyl (DEAM) (Chart 1). Upon metalation the diNHC ligands provide isolable and thermally stable C_1-symmetric palladium, iridium and rhodium catalysts. Unprecedented however, are in situ generated catalysts derived from di-*N*-heterocyclic carbene ligands (diNHC). Herein, we present the first transient formation of a chiral diNHC-supported palladium species capable of efficiently

* Corresponding author. Tel.: +1 352 392 9844; fax: +1 352 392 3255.
E-mail address: veige@chem.ufl.edu (A.S. Veige).

0277-5387/$ - see front matter Published by Elsevier Ltd.
http://dx.doi.org/10.1016/j.poly.2012.07.046

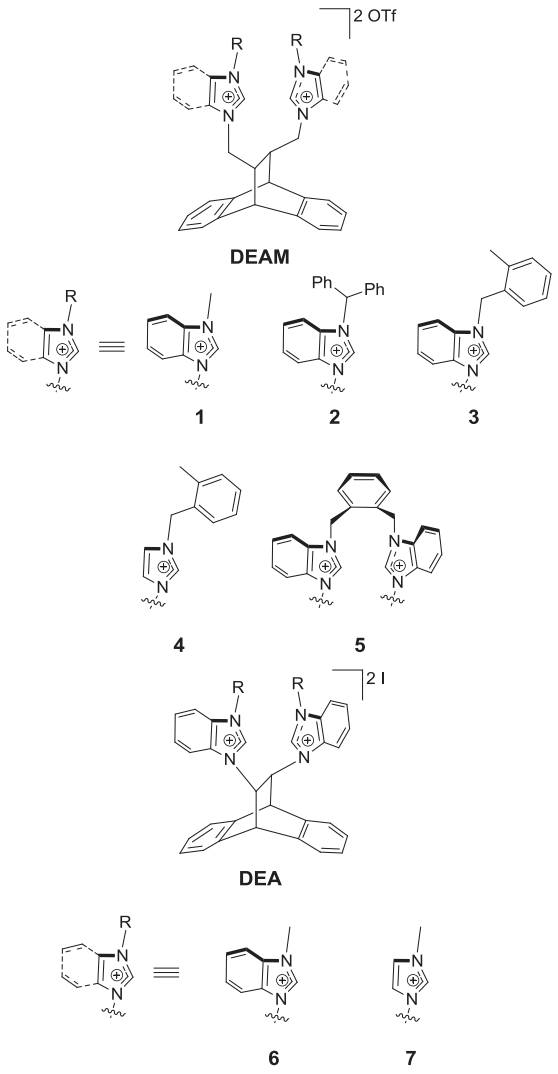

Chart 1. DEAM and DEA ligand precursors.

catalyzing the enantioselective conjugate addition of arylboronic acids to cyclic enones.

2. Experimental

2.1. Materials and methods

Unless specified otherwise, all manipulations were performed under an inert atmosphere using standard glove box techniques. Glassware was oven dried before use. Tetrahydrofuran (THF) was dried using a GlassContours drying column and was degassed using three freeze–pump–thaw cycles before use. $CDCl_3$ was purchased from Cambridge Isotopes dried with calcium hydride and stored over 4 Å molecular sieves. Chloro(allyl)palladium(II) dimer and palladium acetate were purchased from Strem Chemicals Co. and used without further purification. Cesium carbonate, 2-cyclohexen-1-one and 2-cyclopenten-1-one were purchased from Sigma–Aldrich. Boronic acids were purchased from Combi-Blocks Inc. and used without further purification. Diimidazolium ligand precursors **2** [65] and **6** [90] were prepared according to literature methods. Anhydrous potassium carbonate, ether, hexanes, ethyl acetate, THF, dioxane and methanol were purchased from Fischer Scientific and used without further purification. ^1H and $^{13}C\{^1H\}$ NMR spectra were recorded on Varian Mercury broad Band 300 MHz, Varian Mercury 300 MHz, Varian VXR 300 MHz, Gemini 300 MHz and Varian Inova 500 MHz spectrometers. HPLC analysis was done using a Shimadzu prominence instrument with a LC-20AT solvent delivery module, DGU-20A3 degasser, SPD-20A UV–Vis detector (254 nm, 215 nm) and a CBM-20A system controller.

2.1.1. Synthesis of **3**

To an oven dried 100 mL flask containing a stir bar and trans-9,10-dihydro-9,10-ethanoanthracene-11,12-diyldimethanediyl-bis(trifluoromethanesulfonate) [104] (2.52 g, 4.75 mmol) in dry DME (30 mL) was added 1-(2-methylbenzyl)-1*H*-benzimidazole (2.11 g, 9.49 mmol). After refluxing under argon for 1 h, all volatiles were removed in vacuo to provide **3** as a hygroscopic off-white flocculent powder (4.29 g, 93%). ^1H NMR (300 MHz, acetone-d_6): 9.65 (s, 2H, NC*H*N), 8.02 (dd, J = 6 Hz, J = 3 Hz, 2H, NCC*H*CH), 7.96 (dd, J = 9 Hz, J = 3 Hz, 2H, NCC*H*CH), 7.78 (dd, J = 6 Hz, J = 3 Hz, 4H, NCCHC*H*), 7.36–7.21 (m, 12H, aromatic, CHCC*H*CH and CHCCHC*H*, signals overlap), 7.15 (ddd, J = 15 Hz, J = 15 Hz, J = 6 Hz, 4H, CHCCHC*H*), 5.91/5.90 (4H, NCH_2C), 4.76 (dd, J = 15 Hz, J = 3 Hz, 2H, NCH_2CH), 4.42 (s, 2H, CC*H*C), 4.28 (dd, J = 15 Hz, J = 9 Hz, NCH_2CH, 2H), 2.77 (dd, J = 3 Hz, J = 3 Hz, NCH$_2$-C*H*, 2H), 2.45 (s, CH_3, 6H). $^{13}C\{^1H\}$ NMR (75 MHz, acetone-d_6): 143.3 (NCHN), 143.2 (s, NCCH), 140.5 (s, NCCH), 137.8 (quaternary C), 132. 7 (quaternary C), 132.6 (quaternary C), 132.2 (aromatic), 131.9 (quaternary C), 130.0 (aromatic), 129.7 (aromatic), 128.22 (aromatic), 128.19 (aromatic), 127.54 (aromatic), 127.50 (aromatic), 127.20 (aromatic), 126.5 (aromatic), 125.4 (aromatic), 122.1 (q, J = 300 Hz, CF_3), 115.1 (NCCH), 114.9 (NCCH), 51.3 (NCH$_2$-CH), 50.1 (NCH_2C), 45.9 (CCHC), 44.1 (NCH_2CH), 19.3 (CH_3). HR-ESI-FTICR-MS: Calc. for $C_{49}H_{43}N_4SO_3F_3$: m/z 825.3081 [M+SO$_3$-CF_3]$^+$. Found: m/z 825.3020. *Anal.* Calc. for $C_{50}H_{44}N_4S_2O_6F_6$: C, 61.60; H, 4.56; N, 5.75. Found: C, 61.76; H, 4.66; N, 5.41%.

2.1.2. Synthesis of $\mathbf{8}_{exo}/\mathbf{8}_{endo}$

Two solutions are prepared in a glovebox: (A) 500 mg (0.455 mmol) **2** and 310 mg (0.954 mmol) Cs_2CO_3 in 2 mL THF, (B) 86 mg (0.236 mmol) $[Pd(C_3H_5)Cl]_2$ in 3 mL THF. Solution A is stirred for 2 min and B is added at room temperature. Solution AB is then stirred for 16 h at room temperature and then removed from the glovebox. The solution is filtered through a medium fritted funnel and the filtrate is dropped into 35 mL of hexanes. The precipitate is filtered leaving $\mathbf{8}_{exo}/\mathbf{8}_{endo}$ as a white solid (485 mg, 92% yield). Complexes $\mathbf{8}_{exo}/\mathbf{8}_{endo}$ are isolated as a mixture of *endo* and *exo* isomers, thus not all resonances were assigned. MS(HR-ESI-FTICR+): Calc. for $[C_{61}H_{51}N_4Pd]^+$: m/z 945.3164 M$^+$. Found: m/z 945.3172. (*S*,*S*) enantiomer $[\alpha]_D^{20.85}$ −20.593 (c 0.10, CH_2Cl_2), (*R*,*R*) enantiomer $[\alpha]_D^{20.97}$ +24.083 (c 0.10, CH_2Cl_2).

2.1.3. Synthesis of $\mathbf{9}_{exo}/\mathbf{9}_{endo}$

Two solutions are prepared in a glovebox: (A) 500 mg (0.512 mmol) **3** and 351 mg (1.08 mmol) Cs_2CO_3 in 2 mL THF, (B) 94 mg (0.256 mmol) $[Pd(C_3H_5)Cl]_2$ in 3 mL THF. Solution A is stirred for 2 min and B is added at room temperature. Solution AB is then stirred for 16 h at room temperature and then removed from the glovebox. The solution is filtered through a medium fritted funnel and the filtrate is dropped into 35 mL of hexanes. The precipitate is filtered leaving $\mathbf{9}_{exo}/\mathbf{9}_{endo}$ as a white solid (446 mg, 89% yield). Complexes $\mathbf{9}_{exo}/\mathbf{9}_{endo}$ are isolated as a mixture of *endo* and *exo* isomers, thus not all resonances were assigned. Partial assignment of the ^1H and ^{13}C chemical shifts were made in acetone-d_6 at −60 °C, and confirm two isomers (59:31) of a molecule having the two NHC moieties bound to the metal at the C2 position (see Fig. 2 for details). *Anal.* Calc. for $C_{52}H_{47}N_4SPdO_3F_3$: C, 64.29; H, 4.88; N, 5.77. Found: C, 64.25; H, 4.90; N, 5.69%. MS(HR-ESI-FTICR+): Calc. for $[C_{51}$-$H_{47}N_4Pd]^+$: m/z 821.2848. Found: m/z 821.2867. $[\alpha]_D^{20.42}$ −5.799 (c 0.10, CH_2Cl_2).

*2.1.4. Synthesis of **10***

Two solutions are prepared in a glovebox: (**A**) 500 mg (0.455 mmol) **2** and 310 mg (0.954 mmol) Cs_2CO_3 in 2 mL THF, (**B**) 139 mg (0.456 mmol) $Pd(acac)_2$ in 3 mL THF. Solution **A** is stirred for 2 min and **B** is added at room temperature. Solution **AB** is then stirred for 16 h at room temperature and then removed from the glovebox. The solution is filtered through a medium fritted funnel and the filtrate is dropped into 35 mL of hexanes. The precipitate is filtered providing **10** as a pale yellow solid (399 mg, 76% yield). ^{1}H NMR (300 MHz, $CDCl_3$, δ): 8.24 (dd, J = 3 Hz, J = 6 Hz, 1H, aromatic), 8.22 (1H, NC*H*), 7.66 (dd, J = 3 Hz, J = 6 Hz, 2H, aromatic), 7.46–7.13 (m, 21H, NC*H* + aromatic), 7.02–6.90 (m, 5H, aromatic), 6.84–6.75 (m, 3H, aromatic), 6.64 (d, J = 6 Hz, 2H, aromatic), 6.47 (d, J = 9 Hz, 1H, aromatic), 6.14 (dd, J = 6 Hz, J = 6 Hz, 1H, NCH_2CH), 5.98 (d, J = 9 Hz, 2H, aromatic), 5.32 (d, J = 15 Hz, 1H, CH_2), 5.23 (s, 1H, OCC*H*CO), 5.05 (s, 1H, NCH_2CHCH), 4.33 (dd, J = 9 Hz, J = 12 Hz, 1H, CH_2), 4.17 (s, 1H, NCH_2CHCH), 4.13 (dd, J = 9 Hz, J = 12 Hz, 1H, CH_2), 2.64 (d, J = 15 Hz, 1H, CH_2), 2.17 (dd, J = 6 Hz, J = 6 Hz, 1H, NCH_2CH), 1.84 (s, 3H, CH_3), 1.71 (s, 3H, CH_3). ^{13}C{^{1}H} NMR (75 MHz, $CDCl_3$, δ): 187.7 (N*C*N), 186.1 (N*C*N), 167.0 (*C*O), 166.1 (*C*O), 145.0 (NCH_2CHCHC), 143.9 (NCH_2CHCHC), 138.2 (NCH_2CHCHC), 137.7 (NCH_2CHCHC), 137.5 (NCH*C*), 136.0 (NCH*C*), 135.5 (NCH*C*), 135.3 (NCH*C*), 135.2 (NC*C*H), 134.8 (NC*C*H), 133.1 (NC*C*H), 132.3 (NC*C*H), 129.1 (aromatic), 128.6 (aromatic), 128.5 (aromatic), 128.3 (aromatic), 127.9 (aromatic), 127.2 (aromatic), 127.1 (aromatic) 126.4 (aromatic), 126.1 (aromatic), 125.2 (aromatic), 125.1 (aromatic), 124.7 (aromatic), 124.3 (aromatic), 121.7 (aromatic), 115.1 (NC*C*H), 113.8 (NC*C*H), 112.6 (NC*C*H), 109.9 (NC*C*H), 101.0 (OC*C*HCO), 68.3 (N*C*H), 67.9 (N*C*H), 53.2 (NCH_2), 51.3 (NCH_2CH), 50.2 (NCH_2), 46.9 (NCH_2CHCH), 46.6 (NCH_2CHCH), 45.8 (NCH_2CH), 26.5 (CH_3), 26.3 (CH_3). MS(HR-ESI-FTICR+): Calc. for $[C_{63}H_{53}N_4PdO_2]^+$: m/z 1003.3219 M^+. Found: m/z 1003.3252. $[\alpha]_D^{20.23}$ −95.827 (c 0.10, CH_2Cl_2).

*2.1.5. Synthesis of **11***

To a stirring 10 mL THF suspension of the DEA precursor 1,1′-(9,10-dihydro-9,10-ethanoanthracene-11,12-diyl)di(3-methyl-1*H*-imidazol-3-ium) diiodide (**6**) (150 mg, 0.21 mmol) was added palladium acetate (50 mg, 0.22 mmol). The reaction was allowed to stir at room temperature under argon for 5 h, at which point the temperature of the system was increased incrementally in the following manner, for the following durations: 2 h at 40 °C, 2 h at 60 °C, 3 h at 90 °C, and 1 h at 120 °C. The reaction mixture was allowed to cool overnight, with stirring and then solvent was removed in vacuo. On a bench top, the residue was taken up in fresh THF and filtered. The solid remaining on the frit was washed with warm THF until the filtrate was colorless. The volume of the filtrate was reduced to induce crystallization. The product was isolated via filtration as yellow crystals of 11 (70 mg, 37% yield). An alternative procedure for synthesizing **11** involves a similar tiered heating scheme as above, but utilizing DMSO as the solvent. Single crystals amenable to X-ray diffraction were grown from material synthesized in this manner. To a vial containing a very concentrated solution of **11** in DMSO was layered hexanes, and filled with CH_2Cl_2. After 2 days at room temperature, large yellow single crystals were obtained. *Anal.* Calc. for $C_{32}H_{26}I_2N_4Pd{\cdot}THF$: C, 48.10; H, 3.81; N, 6.23. Found: C, 48.19; H, 3.77; N, 6.19%. ^{1}H NMR (499.8 MHz, CD_2Cl_2) δ ppm: 8.77 (d, J = 10.1 Hz, 1H, bridge), 7.82 (d, J = 7.4 Hz, 1H, aromatic), 7.72 (d, J = 7.3 Hz, 1H, aromatic), 7.63–7.59 (m, 2H, aromatic), 7.51 (t, J = 7.5 Hz, 1H, aromatic), 7.40–7.46 (m, 4H, aromatic), 7.30–7.35 (m, 3H, aromatic), 7.18–7.29 (m, 3H, aromatic), 7.13 (m, 1H, aromatic), 5.24 (s, 1H, bridgehead), 5.20 (s, 1H, bridgehead), 4.49 (d, J = 10.1 Hz, 1H, bridge), 4.22 (s, 3H, NCH_3), 3.95 (s, 3H, NCH_3), 3.68 (m, 2H, THF), 1.82 (m, 2H, THF). ^{13}C{^{1}H} NMR (125.69 MHz, CD_2Cl_2) δ (ppm): 177.1 (Pd–*C*), 174.4 (Pd–*C*), 146.7 (C aromatic), 144.8 (C aromatic), 139.0 (C aromatic), 136.6 (C aromatic), 135.9 (C aromatic), 135.7 (C aromatic), 135.1 (C aromatic), 131.7 (C aromatic), 128.5 (C aromatic), 128.2 (C aromatic), 128.0 (C aromatic), 127.7 (C aromatic), 127.4 (C aromatic), 127.3 (C aromatic), 124.9 (C aromatic), 124.3 (C aromatic), 124.2 (C aromatic), 124.1 (C aromatic), 123.9 (C aromatic), 122.33 (C aromatic), 112.3 ($CNCCNCH_3$), 111.6 ($CNCCNCH_3$), 111.5 ($CNCCNCH_3$), 111.2 ($CNCCNCH_3$), 68.2 (THF), 64.3 (s, NCHCH), 62.9 (s, NCHCH), 49.1 (s, NCHCH), 47.4 (s, NCHCH), 39.6 (s, NCH3), 36.0 (s, NCH3), 26.0 (THF). *Anal.* Calc. for $C_{32}H_{26}I_2N_4Pd$ plus one molecule THF: C, 48.10; H, 3.81; N, 6.23. Found: C, 48.19; H, 3.77; N, 6.19%.

2.1.6. Catalysis procedure with in-situ catalyst generation

Under an inert atmosphere, to a 20 mL glass vial was added 5 mol% of the ligand, 12 mol% of base, 2.5 mol% of palladium precursor and THF (1 mL). The reaction was allowed to stir at room temperature for the appropriate time, whereupon 1.5 equiv. of arylboronic acid, base [KOH (33 mol%) or K_2CO_3 (50 mol%)] was added to the vial. Finally, 2-cyclohexen-1-one or 2-cyclopenten-1-one (1 mmol) and degassed water were added to the reaction mixture and the reaction was heated to 68 °C with stirring. One milliliter of saturated sodium bicarbonate was then added and the product was extracted with 10 × 2 mL of diethyl ether. The organic layer was concentrated and the product was purified via column chromatography using 10% EtOAc/hexanes. The yield was measured using ^{1}H NMR spectroscopy and the % e.e. was determined using chiral HPLC.

2.1.7. Catalysis procedure with isolable catalyst

On the bench-top, to a 20 mL glass vial was added 1.5 equiv. of aryl boronic acid, 5 mol% of the catalyst and base (KOH, 33 mol% and K_2CO_3, 50 mol%). Degassed 1 mL of THF/water (10:1) or dioxane/MeOH (4:1) was then added. Finally, 2-cyclohexen-1-one (1 mmol) was added to the reaction mixture and the reaction was heated to 68 °C with stirring. One milliliter of saturated sodium bicarbonate was then added and extracted with 10 × 2 mL of diethyl ether. The organic layer was concentrated and the product was purified via column chromatography using 10% EtOAc/hexanes. The yield was measured using ^{1}H NMR spectroscopy and the % e.e. was determined using chiral HPLC.

2.2. X-ray crystallography

*2.2.1. X-ray experimental details for complexes **8**$_{exo}$/**8**$_{endo}$*

Data are collected at 173 K on a Siemens SMART PLATFORM equipped with a CCD area detector and a graphite monochromator utilizing Mo Kα radiation (λ = 0.71073 Å). Cell parameters are refined using up to 8192 reflections. A full sphere of data (1850 frames) was collected using the ω-scan method (0.3° frame width). The first 50 frames were measured again at the end of data collection to monitor instrument and crystal stability (maximum correction on I is <1%). Absorption corrections by integration are applied based on measured indexed crystal faces. The structure is solved by the Direct Methods in SHELXTL6, and refined using full-matrix least squares. The non-H atoms are treated anisotropically, whereas the hydrogen atoms are calculated in ideal positions and are riding on their respective carbon atoms. The asymmetric unit consists of the Pd complex cation, a triflate anion and a THF molecule. The latter is disordered and could not be modeled properly, thus program SQUEEZE, a part of the PLATON package of crystallographic software, is used to calculate the solvent disorder area and remove its contribution to the overall intensity data. The C19–C21 group is disordered with the middle CH unit occupying two positions. The disordered parts are refined with dependent occupation factors. All atoms of the triflate anion are disordered except the S atom. The final model refines two parts with their site occupation factors fixed at 50%. A total of 650 parameters are refined in the final cycle

of refinement using 8485 reflections with $I > 2\sigma(I)$ to yield R_1 and wR_2 of 5.52% and 14.20%, respectively. Refinement is done using F^2.

2.2.2. X-ray experimental details for complex ***11***

X-Ray intensity data were collected at 100 K on a Bruker DUO diffractometer using Mo Kα radiation (λ = 0.71073 Å) and an APEX-II CCD area detector. Raw data frames were read by program SAINT and integrated using 3D profiling algorithms. The resulting data were reduced to produce *hkl* reflections and their intensities and estimated standard deviations. The data were corrected for Lorentz and polarization effects and numerical absorption corrections were applied based on indexed and measured faces.

The structure was solved and refined in SHELXTL6.1, using full-matrix least-squares refinement. The non-H atoms were refined with anisotropic thermal parameters and all of the H atoms were calculated in idealized positions and refined riding on their parent atoms. The asymmetric unit consists of the Pd complex, a DMSO and 1.5 dichloromethane (DCM) solvent molecules. All solvent molecules were disordered and could not be modeled properly, thus program SQUEEZE, a part of the PLATON package of crystallographic software, was used to calculate the solvent disorder area and remove its contribution to the overall intensity data. The DMSO molecule is disordered in a general position while the DCM molecules are disordered in channels along the *b*-axis. In the final cycle of refinement, 8742 reflections (of which 6698 are observed with $I > 2\sigma(I)$) were used to refine 354 parameters and the resulting R_1, wR_2 and S (goodness of fit) were 2.46%, 4.47% and 0.861, respectively. The refinement was carried out by minimizing the wR_2 function using F^2 rather than F values. R_1 is calculated to provide a reference to the conventional R value but its function is not minimized.

3. Results and discussion

3.1. Synthesis and characterization of isolable catalysts

The purpose of this study is to develop a protocol to generate diNHC–metal catalysts in situ from corresponding diimidazolium salt ligand precursors. To be meaningful, it is important to compare the in situ generated catalyst with isolable versions and compare the difference, if any, on product enantiomeric excess. To accomplish this task, we first synthesized a series of DEAM and DEA diNHC–Pd–L (L = allyl, acetylacetonate, iodide) derivatives (Chart 2).

Treating 0.6 equiv. of $[Pd(C_3H_5)Cl]_2$ with **2** or **3** and 2.2 equiv. Cs_2CO_3 at 25 °C provides $\mathbf{8_{exo}}/\mathbf{8_{endo}}$ and $\mathbf{9_{exo}}/\mathbf{9_{endo}}$ as colorless microcrystalline powders in 92% and 87% yield, respectively. ^{1}H NMR spectra of $\mathbf{8_{exo}}/\mathbf{8_{endo}}$ and $\mathbf{9_{exo}}/\mathbf{9_{endo}}$ reveal signals attributable to two conformers in which the allyl orients *endo* and *exo* with respect to the NHC *N*-substituents. Employing ligand **5** and $[Pd(allyl)Cl]_2$ in a previous study resulted in a similar mixture of isomers [57] (Scheme 1).

A single crystal X-ray diffraction experiment, performed on a crystal comprising a racemic mixture of the compound, confirms the identity of $\mathbf{8_{exo}}/\mathbf{8_{endo}}$. Complexes $\mathbf{8_{exo}}/\mathbf{8_{endo}}$ contain a C_1-symmetric distorted square planar Pd(II) ion coordinated by the diNHC and one η^3-C_3H_5 ligand. The solid state structure reveals a disorder in the central allyl carbon with site occupancies refined to give an *exo* to *endo* ratio of 0.78(1):0.22(1) (Fig. 1, *endo* depicted; see Table 5 for refinement data). Complexes $\mathbf{8_{exo}}/\mathbf{8_{endo}}$ feature a ligand environment comprised entirely of Pd–C bonds. Appropriately, the Pd–NHC bonds are shorter (Pd1–C1 = 2.053(3) and Pd1–C18 =2.086(3) Å) than the Pd–η^3-allyl bonds (Pd1–C19 = 2.162(4), Pd1–C20 = 2.195(4), and Pd–C21 = 2.195(4) Å).

Single crystals of $\mathbf{9_{exo}}/\mathbf{9_{endo}}$ were not obtained; however, partial absolute assignment of the ^{1}H and ^{13}C{^{1}H} chemical shifts

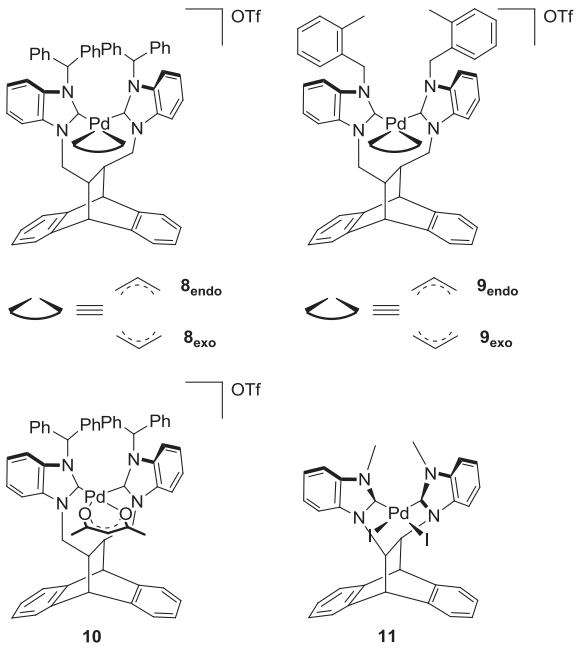

Chart 2. List of new DEAM–Pd and DEA–Pd preformed catalysts employed in this study.

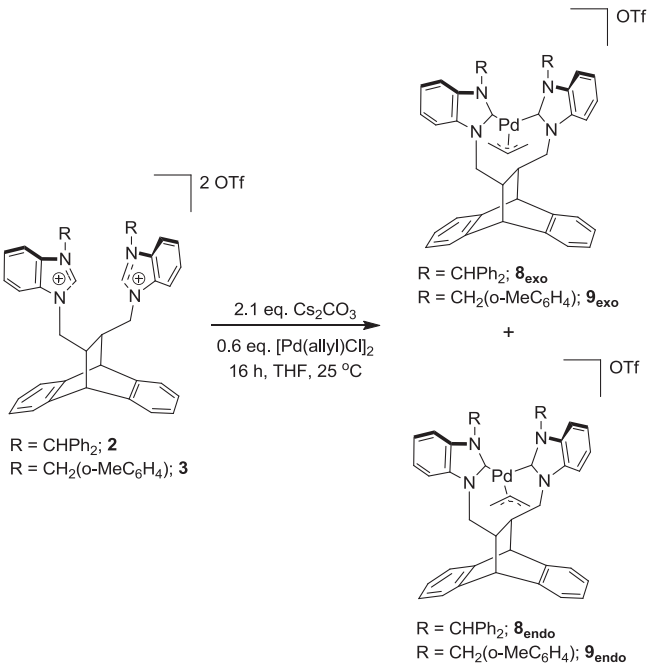

Scheme 1. Synthesis of $\mathbf{8_{endo}}/\mathbf{8_{exo}}$ and $\mathbf{9_{endo}}/\mathbf{9_{exo}}$.

(acetone-d_6 at −60 °C) are possible and confirm the presence of two isomers (59:31). The nOe's observed in a NOESY spectrum did not permit distinction between the exo and endo conformers. Drawing on the structural data of **8** (Fig. 1) and the published data employing ligand **6**, the major isomer is tentatively assigned to $\mathbf{9_{exo}}$. Fig. 2 depicts the NMR data that are conclusively assignable for $\mathbf{9_{exo}}/\mathbf{9_{endo}}$. For example, within the ethanoanthracene unit, the four bridgehead protons for the two conformers (exo: 4.83, 4.39, and endo: 4.89, 4.53 ppm) are identifiable by their long-range coupling with two aromatic carbons at 125 ppm and with two or more quaternary aromatic carbons between 140 and 145 ppm (see ESI). Cross-peaks in a gDQCOSY spectrum enable assignment

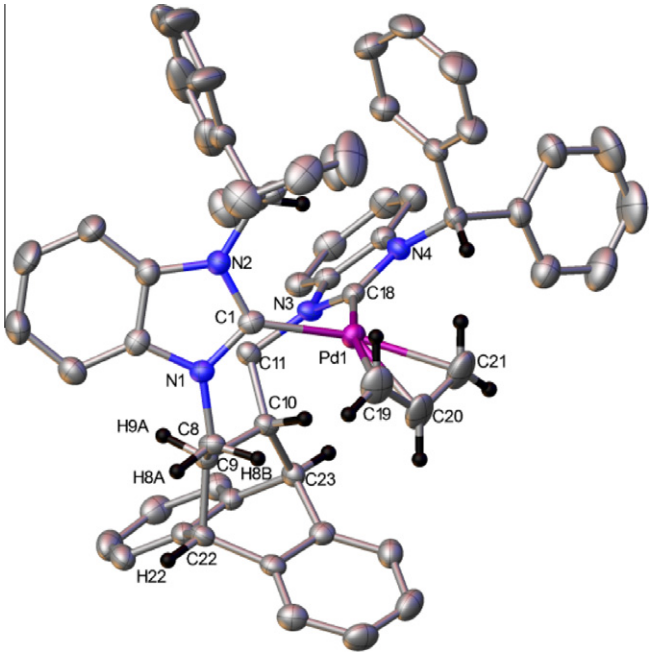

Fig. 1. Molecular structure of DEAM–palladium catalyst $\mathbf{8}_{exo}/\mathbf{8}_{endo}$ ($\mathbf{8}_{exo}$ depicted). Thermal ellipsoids are drawn at the 50% probability level and the OTf^- counter ion and disordered allyl C20′ are removed for clarity. Bond lengths (Å): Pd1–C1 2.053(3), Pd1–C18 2.086(3), Pd1–C20 2.149(6), Pd1–C20′ 2.135(13) (not shown), Pd1–C19 2.162(4), Pd1–C21 2.195(4). Bond angles (°): C1–Pd1–C18 97.14(12), C1–Pd1–C19 95.22(15), C19–Pd–C21 67.28(16), C18–Pd1–C21 100.32(15), C1–Pd1–C21 162.18(15), C18–Pd1–C19 167.60(14).

of the bridge (exo: 4.53, 2.14, and endo: 4.79, 2.28 ppm) and adjacent methylene protons (exo: 3.98/2.93, 5.23/3.58, and endo 4.08/3.07, 5.37/3.81 ppm) for both conformers. A gHMQC experiment allows for the assignment of the corresponding carbons to the above protons. Most importantly, the carbene carbons bound to Pd(II) are uniquely identifiable by their downfield chemical shifts (exo: 186.3, 189.9 ppm, and endo: 186.1, 189.2 ppm), and

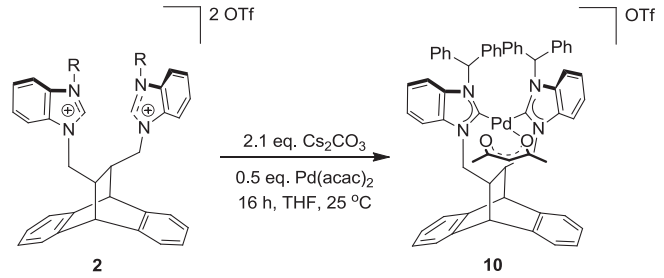

Scheme 2. Synthesis of **10**.

cross-peaks with proximate methylene protons enable their absolute stereochemical assignments. Other cross-peaks to the carbene carbons permit assignment of the benzyl methylene protons (exo: 4.79/5.70, 5.97/5.77, and endo: 5.45/4.82, 5.60/5.60 ppm). Finally, a gDQCOSY experiment identifies the individual allyl protons.

Generating catalysts in situ from various metal precursors will undoubtedly result in the formation of complexes that feature different non-NHC ancillary ligands. Acetylacetonate (acac) is a common ligand found in many metal precursor reagents. Accessing the acac complex **10** as a pale-yellow solid in 79% yield involves treating **2** with 1 equiv. of $Pd(acac)_2$ and 2.1 equiv. of Cs_2CO_3 (Scheme 2) followed by stirring the solution for 12 h, filtration, and precipitation from hexanes. The ^1H and $^{13}C\{^1H\}$ NMR spectra of **10** are indicative of a C_1-symmetric complex. Several unique ^1H NMR resonances support the structure assignment of **10**. The acac methyl proton signals resonate at 1.71 and 1.84 ppm, and the acac methine proton resonates at 5.23 ppm. The ethanoanthracene bridgehead protons resonate at 2.17 and 6.14 ppm with the large 4 ppm difference a consequence of the distinct chiral environment of **10**. One of the diphenylmethine proton signals resonates at 8.22 ppm, while the other proton resonates in a region with several aromatic protons that obscures its exact location. The $^{13}C\{^1H\}$ NMR spectrum also exhibits several diagnostic signals. Notably, the carbene C2 carbons resonate at 187.7 and 186.1 ppm. Signals at 26.3 and 26.5 ppm are attributable to the acac methyl carbons and

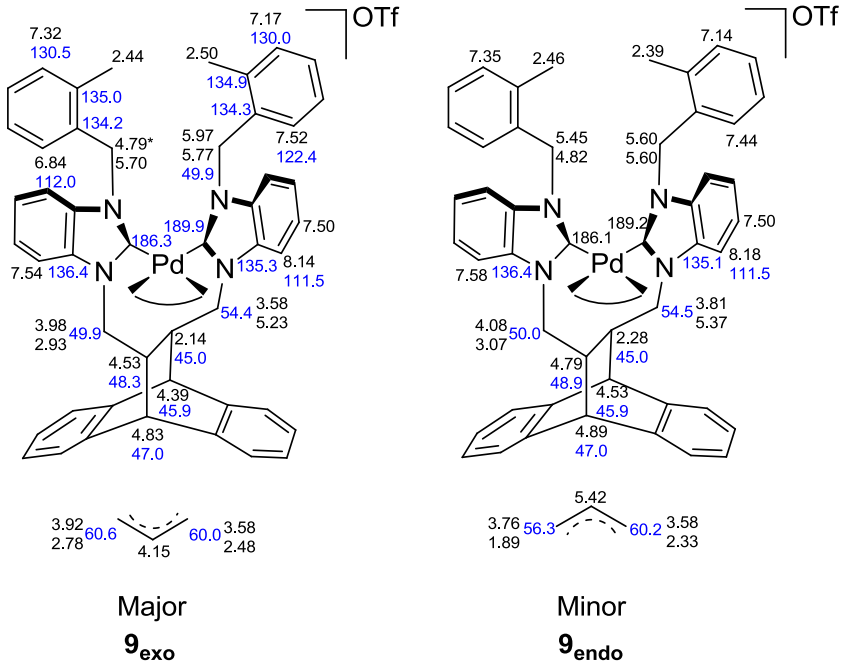

Fig. 2. Partial assignment of the ^1H and $^{13}C\{^1H\}$ NMR data for $\mathbf{9}_{exo}/\mathbf{9}_{endo}$.

the corresponding acac methine resonates at 101.0 ppm. The acac ketone carbons appear in the appropriate region at 167.0 and 166.1 ppm, and the diphenylmethine carbons resonate at 68.3 and 67.9 ppm.

Efforts to synthesize the corresponding DEA–Pd–allyl or Pd–acac derivatives were unsuccessful. Instead, employing a progressive heating method of the ligand precursor **2** and $Pd(OAc)_2$ in THF provides the DEA–PdI_2 complex **11** in 37% yield (Scheme 3). Notably, Hahn et al. [105] and later Özdemir et al. [106] employed this method of progressive heating with $Pd(OAc)_2$ to synthesize other diNHC–palladium complexes. Attempts to simplify the synthesis by heating at 90 or 120 °C alone resulted in either poor yield or no yield. The method seems to be ligand dependant because simply stirring 1,1′-methylene-bis(*N*-methylbenzimidazolyl) diiodide with $Pd(OAc)_2$ in acetonitrile overnight provides the correspond Pd–diiodide biscarbene [107]. A ^1H NMR spectrum of **11** indicates the complex is C_1-symmetric, yielding distinct singlet resonances for the methyl substituent protons at 4.22 ppm and 3.95 ppm. The bridgehead protons appear as singlets at 5.24 ppm and 5.20 ppm and the bridge protons appear as doublets at 8.77 ppm and 4.49 ppm. A large downfield shift of the aliphatic bridge proton H17 (Fig. 3) is attributable to the location of the proton directly beneath the palladium center. Analogous Rh–DEA derivatives exhibit a similar downfield shift [88,90]. Dihedral angles of approximately 78.51° and 80.92° between the two sets of bridge and bridgehead protons results in no observable coupling between the protons, consistent with the vicinal Karplus correlation [108,109].

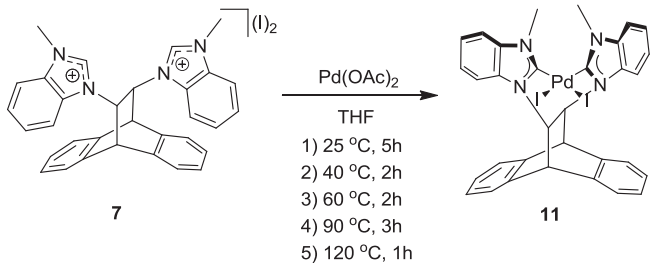

Scheme 3. Synthesis of **11**.

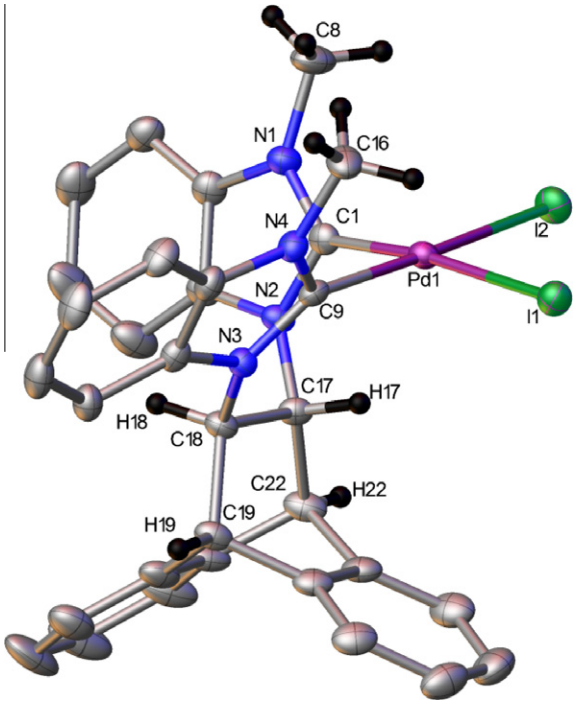

Fig. 3. Molecular structure of **11**. Thermal ellipsoids are shown at the 50% probability level. Bond lengths (Å): Pd1–C1 1.979(3), Pd1–C9 2.013(3), Pd1–I1 2.6528(5), Pd1–I2 2.6410(5). Bond angles (°): C1–Pd1–C9 86.75(10), C1–Pd1–I2 86.85(7), C9–Pd1–I1 91.48(7), I1–Pd1–I2 94.813(11).

Single crystals grow by slowly diffusing CH_2Cl_2 into a concentrated solution of a racemic mixture of **11** in DMSO/hexanes. Fig. 3 depicts the structure and Table 5 lists refinement data from a single crystal X-ray diffraction experiment and confirms the molecular structure of **11**. The neutral complex comprises a slightly distorted square-planar Pd(II) center chelated by the diNHC ligand and *cis*-iodides. Evidence for the DEA ligand providing a more constrained coordination environment than the related DEAM counterparts is the much smaller NHC–Pd–NHC angle of 86.75(10)° compared to 97.14(12)° found in the DEAM–Pd–η^3-allyl complex $\mathbf{8_{exo}}/\mathbf{8_{endo}}$. Despite the strain, **11** contains shorter Pd–NHC distances (Pd1–C1 1.979(3) and Pd1–C9 2.013(3) Å) than in $\mathbf{8_{exo}}/\mathbf{8_{endo}}$, a consequence perhaps of the much weaker *trans*-influence of an iodide versus an η^3-allyl ligand.

3.2. Catalytic arylboronic acid addition to enones with isolated diNHC–Pd complexes

Isolated catalysts $\mathbf{8_{exo}}/\mathbf{8_{endo}}$ and the reaction of 2-cyclohexen-1-one with phenylboronic acid were chosen to standardize reaction conditions. Solvent and base screening experiments indicate that dioxane/methanol and K_2CO_3 yield optimal results in terms of yield and enantioselectivity (Table 1, entry 4). The solvent combination of THF/H_2O provides slightly lower % e.e. (Table 1, entries 5–7). Employing KOH as the base provided either no enantiomeric enrichment or in one case 34% (Table 1, entry 3). The conclusion from this study is that no single set of conditions were found that significantly enhanced the % e.e.; as a consequence both bases and solvent systems were employed in subsequent screening studies.

Employing the isolable catalysts in Chart 1 provides two important results. Notably, the more constrained DEA ligand in complex **11** does not turnover the reaction. This is surprising since the related Rh(I) version with cyclooctadiene as counter ligand provides 82% e.e. [44,88]. Employing either $\mathbf{8_{exo}}/\mathbf{8_{endo}}$ or $\mathbf{9_{exo}}/\mathbf{9_{endo}}$ did not significantly improve the % e.e.; for example, complex $\mathbf{9_{exo}}/\mathbf{9_{endo}}$ yields 44% e.e. (Table 2, entry 2). Moreover, the DEAM–Pd–acac complex **10** is not active at 35 °C and must be heated to 80 °C for

Table 1
Optimization of base and solvent.

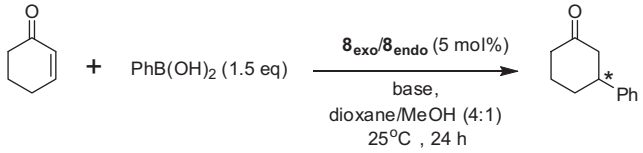

Entry	Base (mol%)	Solvent combination	% Yield[a]	% e.e.[b]
1	None	dioxane:MeOH(4:1)	0	0
2	KOH(25)	dioxane:MeOH(4:1)	73	34(R)
3	KOH(50)	dioxane:MeOH(4:1)	>98	0
4	K_2CO_3(50)	dioxane:MeOH(4:1)	>98	46(R)
5	KOH(50)	THF:H_2O(10:1)	>98	20(R)
6	KOH(40)	THF:H_2O(10:1)	>98	29(R)
7	K_2CO_3(40)	THF:H_2O(10:1)	>98	38(R)
8[c]	KOH(40)	THF:H_2O(10:1)	0	0
9[c]	K_2CO_3(50)	dioxane:MeOH(4:1)	0	0

[a] NMR yield.
[b] Enantiomer in parenthesis, determined by HPLC.
[c] T = 0 °C.

Table 2
Catalyst optimization using pre-formed catalysts..

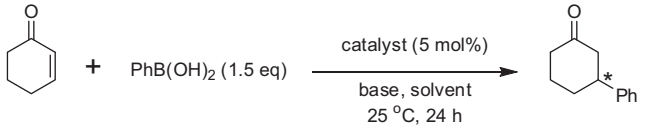

Entry	Base	Catalyst	Time (h)	% Yield[a]	% e.e.[b]
1	K_2CO_3(50)	(S,S)-**9**	18	>98	11(R)
2	K_2CO_3(50)	(S,S)-**8**	24	>98	46(R)
3[c]	K_2CO_3(50)	(S,S)-**8**	24	95	44(R)
4[d]	K_2CO_3(50)	(S,S)-**8**	24	95	40–60(R)
5[e]	KOH(40)	(S,S)-**10**	18	0	0
6[f]	KOH(40)	(S,S)-**10**	18	50	0

[a] NMR yield.
[b] Enantiomer in parenthesis, determined by HPLC.
[c] 4-Fluorophenylboronic acid.
[d] 2-Naphthylboronic acid, e.e. estimated.
[e] T = 50 °C, THF:H_2O(10:1).
[f] T = 80 °C, THF:H_2O(10:1).

Table 3
Palladium precursor screening with ligands **2**, **3**, and **6**.

Entry	Ligand	Metal precursor	Solvent	Base	% Yield[a]
1	**2**	$Pd(BzCN)_2Cl_2$	THF:H_2O	Cs_2CO_3	–
2	**2**	$[Pd(allyl)Cl]_2$	THF:H_2O	Cs_2CO_3	–
3	**2**	$Pd(OAc)_2$	THF:H_2O	Cs_2CO_3	>98
4	**2**	$Pd(OAc)_2$	dioxane:MeOH	Cs_2CO_3	–
5	**2**	$Pd(OAc)_2$	THF:H_2O	KHMDS	–
6	**2**	$Pd(OAc)_2$	THF:H_2O	KO^{t}Bu	–
7	**3**	$Pd(BzCN)_2Cl_2$	THF:H_2O	Cs_2CO_3	–
8	**3**	$[Pd(allyl)Cl]_2$	THF:H_2O	Cs_2CO_3	–
9	**3**	$Pd(OAc)_2$	THF:H_2O	Cs_2CO_3	–
10	**3**	$Pd(OAc)_2$	dioxane:MeOH	Cs_2CO_3	–
11	**3**	$Pd(OAc)_2$	THF:H_2O	KHMDS	–
12	**3**	$Pd(OAc)_2$	THF:H_2O	KO^{t}Bu	–
13	**6**	$Pd(BzCN)_2Cl_2$	THF:H_2O	Cs_2CO_3	–
14	**6**	$[Pd(allyl)Cl]_2$	THF:H_2O	Cs_2CO_3	10
15	**6**	$Pd(OAc)_2$	THF:H_2O	Cs_2CO_3	–
16	**6**	$Pd(OAc)_2$	dioxane:MeOH	Cs_2CO_3	–
17	**6**	$Pd(OAc)_2$	THF:H_2O	KHMDS	–
18	**6**	$Pd(OAc)_2$	THF:H_2O	KO^{t}Bu	–

[a] NMR yield, allyl = η^3-BzCN = benzonitrile, OAc = acetate.

product formation to be observed, but the % e.e. = 0 (Table 2, entry 9).

Table 4
Asymmetric conjugate addition of boronic acids to cyclic enones using in-situ generated catalyst **12**.

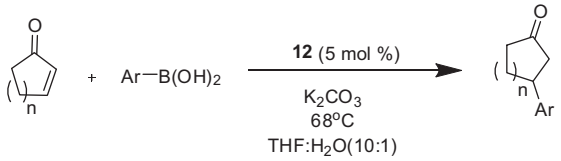

Entry	n	Ar	% Yield[a]	% e.e.[b]
1	1	C_6H_5	87	c
2	1	2-$CH_3C_6H_4$	36	50(R)
3	1	2-$CH_3OC_6H_4$	35	51(R)
4	1	4-$CH_3OC_6H_4$	30	35(R)
5	1	1-naphthyl	24	30(R)
6	1	2-$CF_3C_6H_4$	16	d
7	1	2-FC_6H_4	0	–
8	1	4-FC_6H_4	0	–
9	1	2,6-di$CH_3C_6H_3$	0	–
10	2	C_6H_5	98	51(R)
11	2	2-$CH_3C_6H_4$	62	33(R)
12	2	1-naphthyl	48	30(R)
13	2	2-$CF_3C_6H_4$	0	–
14	2	2-FC_6H_4	0	–
15	2	4-FC_6H_4	0	–
16	2	2,6-diFC_6H_3	0	–

[a] NMR yield.
[b] HPLC.
[c] Enantiomers could not be separated by HPLC.
[d] Product could not be separated from reaction mixture.

3.3. Catalytic arylboronic acid addition to enones with in situ generated diNHC–Pd complexes

Employing the ligand precursor **2**, reactions were screened to find the ideal conditions to generate a catalyst in situ. The method involves heating the ligand precursor diimidazolium salt with a Pd source followed by substrate addition. Palladium acetate ($Pd(OAc)_2$) proved to be the best metal precursor. Other palladium reagents including palladium bis(benzonitrile)dichloride and palladium(allyl)chloride dimer do not generate active catalysts (Table 3, entries 1 and 2). Other than cesium carbonate, bases such as potassium hexamethyldisilazide and potassium *tert*-butoxide were screened, but the catalytic results were poor (Table 3, entries 5 and 6) (Scheme 4).

Optimal conditions require palladium acetate, ligand precursor **2**, and cesium carbonate at 25 °C (Table 3, entry 3). In fact, the yield is >98% and the % e.e. is essentially identical to the corresponding

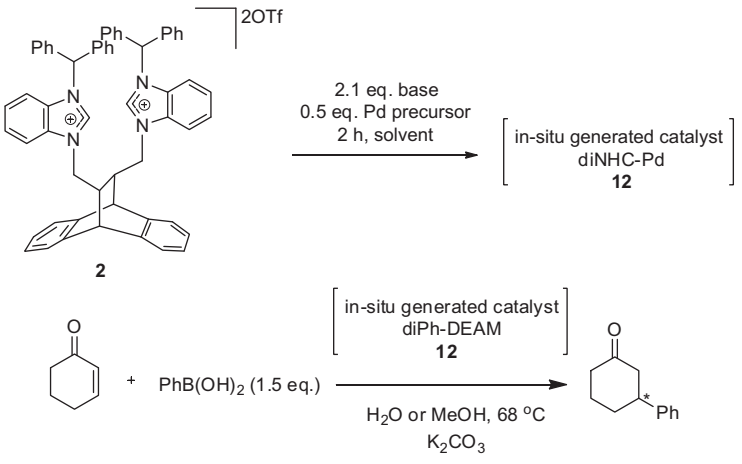

Scheme 4. Method for generating an active diNHC–Pd–L complex in situ and subsequent catalysis.

Table 5
Crystallographic data for **8** and **11**.

Complex	**8**	**11**
Empirical formula	$C_{66}H_{59}N_4PdF_3O_3S$	$C_{35.50}H_{35}Cl_3I_2N_4OPdS$
Formula weight	1151.63	1032.29
T (K)	173(2)	100(2)
λ (Å)	0.71073	0.71073
Crystal system	monoclinic	triclinic
Space group	$P2(1)/c$	$P\bar{1}$
a (Å)	11.2878(8)	12.1289(19)
b (Å)	26.8378(19)	13.523(2)
c (Å)	18.4977(13)	14.568(2)
α (°)	90	115.711(2)
β (°)	96.4820(10)	97.645(3)
γ (°)	90	109.958(2)
V (Å^3)	5567.9(7)	1908.7(5)
Z	4	2
ρ_{calc} (mg mm^{-3})	1.374	1.796
Crystal size (mm^3)	0.19 x 0.19 x 0.08	0.09 x 0.07 x 0.02
Absorption coefficient (mm^{-1})	0.432	2.402
$F(000)$	2384	1006
θ range for data collection (°)	1.48–27.50	1.64–27.50
Limiting indices	$-14 \leqslant h \leqslant 14$, $-31 \leqslant k \leqslant 34$, $-24 \leqslant l \leqslant 24$	$-15 \leqslant h \leqslant 15$, $-17 \leqslant k \leqslant 17$, $-18 \leqslant l \leqslant 18$
Number of reflections collected	37 347	23 289
Number of independent reflections (R_{int})	12 743 (0.9224)	8742(0.0344)
Completeness to θ = 27.50° (%)	99.7	99.8
Absorption correction	integration	numerical
Refinement method	Full-matrix least-squares on F^2	Full-matrix least-squares on F^2
Data/restraints/parameters	12 743/60/650	8742/0/354
R_1,[a] wR_2[b] [$I > 2\sigma(I)$]	0.0552, 0.1420	0.0246, 0.0447 [6698]
R_1,[a] wR_2[b] (all data)	0.0853, 0.1522	0.0356, 0.0461
GOF[c] on F^2	0.984	0.861
Largest difference in peak and hole (e Å^{-3})	1.101 and −1.002	0.667 and −0.699

[a] $R_1 = \Sigma||F_o| - |F_c||/\Sigma|F_o|$.
[b] $wR_2 = (\Sigma(w(F_o^2 - F_c^2)^2)/\Sigma(w(F_o^2)^2))^{1/2}$.
[c] GOF = $(\Sigma w(F_o^2 - F_c^2)^2/(n-p))^{1/2}$. $w = 1/[\sigma^2(F_o^2)+(m*p)^2 + n*p]$, $p = [\max(F_o^2,0) + 2*F_c^2]/3$, m and n are constants.

isolated catalyst $\mathbf{8_{exo}}/\mathbf{8_{endo}}$. To maximize efficiency, the induction time to generate the active catalyst was also examined. The reaction mixture was allowed to stir for different durations (0.5, 2, 6, and 8 h) prior to substrate addition. The ideal time for catalyst generation is 2 h. Two additional diimidazolium ligand precursors (**3** and **6**) were screened but the results indicate no active catalysts form (Table 3, entries 7–18). The only combination that results in product formation (10% yield) is ligand **6** and $[Pd(allyl)Cl]_2$.

Next, various substrates were screened to elucidate the functional group tolerance of the in situ catalyst (Table 4). From the results listed in Table 4 it is apparent the substrates can be separated into two classes: boronic acids containing electron-donating aryl groups, and boronic acids containing electron-withdrawing aryl groups. Electronically donating aryl groups on the boronic acid form product in low yields and modest to low % e.e., while electron-withdrawing fluoro-substituted arenes provide no yield, except in one case 16% yield was obtained for 2-$CF_3C_6H_4$-$B(OH)_2$. Introduction of a single electron-withdrawing substituent retards the reaction. Considering the arylboronic acid acts as a nucleophile in the mechanism, the poor performance of fluorinated substrates is understandable. The maximum % e.e. of ~50% was obtained for Ar-$B(OH)_2$, where Ar = 2-$CH_3C_6H_4$ (n = 1), 2-$CH_3OC_6H_4$ (n = 1), and C_6H_5 (n = 2).

4. Conclusions

Straightforward, efficient, and cost effective access to chiral catalysts is important for rapid screening of catalyst activity and enantioselectivity. Simple addition of a chiral auxiliary (ligand) to a metal ion precursor to generate an active catalyst in situ eliminates costly catalyst preparation steps and associated waste products. In the case of NHC ligands, due to the common technique of employing transmetalating reagents, such as Ag^+, an in situ approach is particularly inviting. However, methods are not well developed for creating catalysts in situ from diimidazolium salt precursors. A major conclusion from this study is that establishing a general set of conditions, even for a very specific class of ligand, would be difficult. Results within Table 3 indicate only one set of conditions results in an active catalyst, despite the fact ligand precursors **2** and **3** only differ in their *N*-substituent group (**2** = diphenylmethine, and **3** = *o*-methylbenzyl). Clearly, small changes in ligand structure dictate whether a catalyst forms in situ and is active. Moreover, the conditions are rather specific. Employing ligand **2,** a catalysts forms only in the presence of $Pd(OAc)_2$, THF/H_2O and Cs_2CO_3 in conjunction with a carefully regulated heating regimen. Other variations do not result in an active catalyst. Thus, it seems likely the perfect conditions could be overlooked. Despite the fact a clear trend was not elucidated in this study, an active catalyst was generated in situ from diimidazolium salt **2** and the inexpensive metal precursor $Pd(OAc)_2$. The different anionic ancillary ligands bound to the Pd(II) ion may account for the difference in activity between the catalysts generated in situ and the isolable versions. For the in situ catalyst acetate is likely the ancillary ligand, whereas for **8**, **10**, and **11**, they are iodide, acetylacetonate, and allyl, respectively.

Though the enantioselectivities obtained for the boronic acid addition to enones were low, this is consistent with previous results employing isolable catalysts, and was not unexpected [65,88]. The positive outcome from this study is that the discovery of a method to generate a catalyst in situ will allow more rapid screening of other enantioselective reaction types to find a class of reactions that better suites the inherent DEAM and DEA ligand chiral environment.

Acknowledgments

The authors thank UF for financial support. A.S.V. is the recipient of an Alfred P. Sloan Fellowship (2010–2012). K.A.A. thanks the NSF (CHE-0821346) and UF for funding the purchase of X-ray equipment. Research quantities of the DEAM and DEA ligands are available for purchase from Strem Chemicals Inc.

Appendix A. Supplementary data

CCDC 886187 and 886186 contain the supplementary crystallographic data for **8** and **11**, respectively. These data can be obtained free of charge via http://www.ccdc.cam.ac.uk/conts/retrieving.html, or from the Cambridge Crystallographic Data Centre, 12 Union Road, Cambridge CB2 1EZ, UK; fax: (+44) 1223-336-033; or e-mail: deposit@ccdc.cam.ac.uk. Supplementary data associated with this article can be found, in the online version, at http://dx.doi.org/10.1016/j.poly.2012.07.046.

References

[1] T. Dröge, F. Glorius, Angew. Chem., Int. Ed. 49 (2010) 6940.
[2] S. Diez-Gonzalez, N. Marion, S.P. Nolan, Chem. Rev. 109 (2009) 3612.
[3] H. Jacobsen, A. Correa, A. Poater, C. Costabile, L. Cavallo, Coord. Chem. Rev. 253 (2009) 687.
[4] D.R. Snead, H. Seo, S. Hong, Curr. Org. Chem. 12 (2008) 1370.
[5] F.E. Hahn, M.C. Jahnke, Angew. Chem., Int. Ed. 47 (2008) 3122.
[6] R.E. Douthwaite, Coord. Chem. Rev. 251 (2007) 702.
[7] R.H. Crabtree, Coord. Chem. Rev. 251 (2007) 595.
[8] C.M. Crudden, D.P. Allen, Coord. Chem. Rev. 248 (2004) 2247.
[9] V. Cesar, S. Bellemin-Laponnaz, L.H. Gade, Chem. Soc. Rev. 33 (2004) 619.
[10] M.C. Perry, K. Burgess, Tetrahedron: Asymmetry 14 (2003) 951.
[11] W.A. Herrmann, Angew. Chem., Int. Ed. 41 (2002) 1290.
[12] H. Clavier, S.P. Nolan, Chem. Commun. 46 (2010) 841.
[13] L. Cavallo, A. Poater, B. Cosenza, A. Correa, S. Giudice, F. Ragone, V. Scarano, Eur. J. Inorg. Chem. (2009) 1759.
[14] A. Fürstner, M. Alcarazo, H. Krause, C.W. Lehmann, J. Am. Chem. Soc. 129 (2007) 12676. and references therein.
[15] A.C. Hillier, W.J. Sommer, B.S. Yong, J.L. Petersen, L. Cavallo, S.P. Nolan, Organometallics 22 (2003) 4323.
[16] A.R. Chianese, X.W. Li, M.C. Janzen, J.W. Faller, R.H. Crabtree, Organometallics 22 (2003) 1663.
[17] M. Alcarazo, T. Stork, A. Anoop, W. Thiel, A. Fürstner, Angew. Chem., Int. Ed. 49 (2010) 2542.
[18] D.M. Khramov, V.M. Lynch, C.W. Bielawski, Organometallics 26 (2007) 6042.
[19] S. Fantasia, J.L. Petersen, H. Jacobsen, L. Cavallo, S.P. Nolan, Organometallics 26 (2007) 5880.
[20] H. Jacobsen, A. Correa, C. Costabile, L. Cavallo, J. Organomet. Chem. 691 (2006) 4350.
[21] M.D. Sanderson, J.W. Kamplain, C.W. Bielawski, J. Am. Chem. Soc. 128 (2006) 16514.
[22] L. Mercs, G. Labat, A. Neels, A. Ehlers, M. Albrecht, Organometallics 25 (2006) 5648.
[23] X.L. Hu, I. Castro-Rodriguez, K. Olsen, K. Meyer, Organometallics 23 (2004) 755.
[24] H. Nakai, X.L. Hu, L.N. Zakharov, A.L. Rheingold, K. Meyer, Inorg. Chem. 43 (2004) 855.
[25] D. Nemcsok, K. Wichmann, G. Frenking, Organometallics 23 (2004) 3640.
[26] X.L. Hu, Y.J. Tang, P. Gantzel, K. Meyer, Organometallics 22 (2003) 612.
[27] J.C. Green, R.G. Scurr, P.L. Arnold, F.G.N. Cloke, Chem. Commun. (1997) 1963.
[28] G. Buscemi, M. Basato, A. Biffis, A. Gennaro, A.A. Isse, M.M. Natile, C. Tubaro, J. Organomet. Chem. 695 (2010) 2359.
[29] H. Plenio, V. Sashuk, L.H. Peeck, Chem. Eur. J. 16 (2010) 3983.
[30] N.M. Scott, H. Clavier, P. Mahjoor, E.D. Stevens, S.P. Nolan, Organometallics 27 (2008) 3181.
[31] R.A. Kelly, H. Clavier, S. Giudice, N.M. Scott, E.D. Stevens, J. Bordner, I. Samardjiev, C.D. Hoff, L. Cavallo, S.P. Nolan, Organometallics 27 (2008) 202.
[32] C.M. Thiele, S. Leuthausser, V. Schmidts, H. Plenio, Chem. Eur. J. 14 (2008) 5465.
[33] H. Plenio, S. Leuthausser, D. Schwarz, Chem. Eur. J. 13 (2007) 7195.
[34] S.P. Nolan, *N*-Heterocyclic Carbenes in Synthesis, Wiley-VHC, Weinheim, 2006.
[35] W.A. Herrmann, J. Schütz, G.D. Frey, E. Herdtweck, Organometallics 25 (2006) 2437.
[36] R. Dorta, E.D. Stevens, N.M. Scott, C. Costabile, L. Cavallo, C.D. Hoff, S.P. Nolan, J. Am. Chem. Soc. 127 (2005) 2485.
[37] M. Süβner, H. Plenio, Chem. Commun. (2005) 5417.
[38] R. Dorta, E.D. Stevens, C.D. Hoff, S.P. Nolan, J. Am. Chem. Soc. 125 (2003) 10490.
[39] K. Denk, P. Sirsch, W.A. Herrmann, J. Organomet. Chem. 649 (2002) 219.
[40] J.K. Huang, E.D. Stevens, S.P. Nolan, J.L. Petersen, J. Am. Chem. Soc. 121 (1999) 2674.
[41] J.K. Huang, H.J. Schanz, E.D. Stevens, S.P. Nolan, Organometallics 18 (1999) 2370.
[42] C. Köcher, W.A. Herrmann, J. Organomet. Chem. 532 (1997) 261.
[43] A.B.P. Lever, Inorg. Chem. 29 (1990) 1271.
[44] M.S. Jeletic, C.E. Lower, I. Ghiviriga, A.S. Veige, Organometallics 30 (2011) 6034.
[45] L. Cavallo, F. Ragone, A. Poater, J. Am. Chem. Soc. 132 (2010) 4249.
[46] F. Glorius, S. Wurtz, Acc. Chem. Res. 41 (2008) 1523.
[47] V. Lavallo, Y. Canac, C. Präsang, B. Donnadieu, G. Bertrand, Angew. Chem., Int. Ed. 44 (2005) 5705.
[48] F.J. Wang, L.J. Liu, W.F. Wang, S.K. Li, M. Shi, Coord. Chem. Rev. 256 (2012) 804.
[49] G.W. Shigeng, J.K. Tang, D. Zhang, Q.R. Wang, Z.X. Chen, L.H. Weng, J. Organomet. Chem. 700 (2012) 223.
[50] S.K.U. Riederer, B. Bechlars, W.A. Herrmann, F.E. Kuhn, Dalton Trans. 40 (2011) 41.
[51] Z. Liu, P. Gu, M. Shi, P. McDowell, G.G. Li, Org. Lett. 13 (2011) 2314.
[52] Z. Liu, P. Gu, M. Shi, Chem. Eur. J. 17 (2011) 5796.
[53] L.J. Liu, F. Wang, W. Wang, M.X. Zhao, M. Shi, Beilstein J. Org. Chem. 7 (2011) 555.
[54] Q. Xu, R. Zhang, T. Zhang, M. Shi, J. Org. Chem. 75 (2010) 3935.
[55] Z. Liu, M. Shi, Tetrahedron 66 (2010) 2619.
[56] Z. Liu, M. Shi, Organometallics 29 (2010) 2831.
[57] M.S. Jeletic, I. Ghiviriga, K.A. Abboud, A.S. Veige, Dalton Trans. 39 (2010) 6392.
[58] S.H. Cao, M. Shi, Tetrahedron: Asymmetry 21 (2010) 2675.
[59] A. Arnanz, C. Gonzalez-Arellano, A. Juan, G. Villaverde, A. Corma, M. Iglesias, F. Sanchez, Chem. Commun. 46 (2010) 3001.
[60] W.F. Wang, T. Zhang, M. Shi, Organometallics 28 (2009) 2640.
[61] G.N. Ma, T. Zhang, M. Shi, Org. Lett. 11 (2009) 875.
[62] Z. Liu, M. Shi, Tetrahedron: Asymmetry 20 (2009) 119.
[63] S.J. Liu, L.J. Liu, M. Shi, Appl. Organomet. Chem. 23 (2009) 183.
[64] L.J. Liu, F.J. Wang, M. Shi, Organometallics 28 (2009) 4416.
[65] M.S. Jeletic, M.T. Jan, I. Ghiviriga, K.A. Abboud, A.S. Veige, Dalton Trans. (2009) 2764.
[66] T. Zhang, M. Shi, M.X. Zhao, Tetrahedron 64 (2008) 2412.
[67] T. Zhang, M. Shi, Chem. Eur. J. 14 (2008) 3759.
[68] Q. Xu, X.X. Gu, S.J. Liu, Q.Y. Dou, M. Shi, J. Org. Chem. 72 (2007) 2240.
[69] A.R. Chianese, R.H. Crabtree, Organometallics 24 (2005) 4432.
[70] H.B. Song, Y.Q. Liu, D.N. Fan, G.F. Zi, J. Organomet. Chem. 696 (2011) 3714.
[71] T.P. Yoon, E.N. Jacobsen, Science 299 (2003) 1691.
[72] C.L. Yang, S.P. Nolan, Organometallics 21 (2002) 1020.
[73] H.M. Lee, S.P. Nolan, Org. Lett. 2 (2000) 2053.
[74] C.M. Zhang, J.K. Huang, M.L. Trudell, S.P. Nolan, J. Org. Chem. 64 (1999) 3804.
[75] J.K. Huang, S.P. Nolan, J. Am. Chem. Soc. 121 (1999) 9889.
[76] F. Gini, B. Hessen, A.J. Minnaard, Org. Lett. 7 (2005) 5309.
[77] K. Okamoto, T. Hayashi, V.H. Rawal, Org. Lett. 10 (2008) 4387.
[78] J.G. Boiteau, R. Imbos, A.J. Minnaard, B.L. Feringa, Org. Lett. 5 (2003) 1385.
[79] J.-G. Boiteau, R. Imbos, A.J. Minnaard, B.L. Feringa, Org. Lett. 5 (2003) 681.
[80] X.Q. Feng, Y.Z. Wang, B.B. Wei, J. Yang, H.F. Du, Org. Lett. 13 (2011) 3300.
[81] F. Gini, B. Hessen, B.L. Feringa, A.J. Minnaard, Chem. Commun. (2007) 710.
[82] S. Oi, A. Taira, Y. Honma, T. Sato, Y. Inoue, Tetrahedron: Asymmetry 17 (2006) 598.
[83] C.L. Winn, F. Guillen, J. Pytkowicz, S. Roland, P. Mangeney, A. Alexakis, J. Organomet. Chem. 690 (2005) 5672.
[84] R. Itooka, Y. Iguchi, N. Miyaura, J. Org. Chem. 68 (2003) 6000.
[85] T. Hayashi, K. Yamasaki, Chem. Rev. 103 (2003) 2829.
[86] F. Guillen, C.L. Winn, A. Alexakis, Tetrahedron: Asymmetry 12 (2001) 2083.
[87] S. Sakuma, M. Sakai, R. Itooka, N. Miyaura, J. Org. Chem. 65 (2000) 5951.
[88] M.S. Jeletic, R.J. Lowry, J.M. Swails, I. Ghiviriga, A.S. Veige, J. Organomet. Chem. 696 (2011) 3127.
[89] R.J. Lowry, M.T. Jan, K.A. Abboud, I. Ghiviriga, A.S. Veige, Polyhedron 29 (2010) 553.
[90] R.J. Lowry, M.K. Veige, O. Clement, K.A. Abboud, I. Ghiviriga, A.S. Veige, Organometallics 27 (2008) 5184.
[91] M.S. Jeletic, I. Ghiviriga, K.A. Abboud, A.S. Veige, Organometallics 26 (2007) 5267.
[92] S. Anezaki, Y. Yamaguchi, M. Asami, Chem. Lett. 39 (2010) 398.
[93] A. Meyer, M.A. Taige, T. Strassner, J. Organomet. Chem. 694 (2009) 1861.
[94] U. Nagel, C. Diez, Eur. J. Inorg. Chem. (2009) 1248.
[95] H. Clavier, J.C. Guillemin, M. Mauduit, Chirality 19 (2007) 471.
[96] S.K. Schneider, J. Schwarz, G.D. Frey, E. Herdtweck, W.A. Herrmann, J. Organomet. Chem. 692 (2007) 4560.
[97] C. Marshall, M.F. Ward, W.T.A. Harrison, J. Organomet. Chem. 690 (2005) 3970.
[98] M. Shi, W.L. Duan, Appl. Organomet. Chem. 19 (2005) 40.
[99] C. Marshall, M.F. Ward, W.T.A. Harrison, Tetrahedron Lett. 45 (2004) 5703.
[100] W.L. Duan, M. Shi, G.B. Rong, Chem. Commun. (2003) 2916.
[101] L.G. Bonnet, R.E. Douthwaite, R. Hodgson, Organometallics 22 (2003) 4384.
[102] D.S. Clyne, J. Jin, E. Genest, J.C. Gallucci, T.V. RajanBabu, Org. Lett. 2 (2000) 1125.
[103] C.M. Zhang, M.L. Trudell, Tetrahedron Lett. 41 (2000) 595.
[104] K.L. Gibis, G. Helmchen, G. Huttner, L. Zsolnai, J. Organomet. Chem. 445 (1993) 181.

[105] F.E. Hahn, M.C. Jahnke, V. Gomez-Benitez, D. Morales-Morales, T. Pape, Organometallics 24 (2005) 6458.
[106] I. Özdemir, S. Demir, O. Sahin, O. Buyukgungor, B. Cetinkaya, J. Organomet. Chem. 695 (2010) 1555.
[107] F.E. Hahn, M. Foth, J. Organomet. Chem. 585 (1999) 241.
[108] M. Karplus, J. Chem. Phys. 30 (1959) 11.
[109] M. Karplus, J. Am. Chem. Soc. 85 (1963) 2870.